Jpn. J. Appl. Phys. Vol. 40 (2001) pp. 3801–3806
Part 1, No. 5B, May 2001

Fundamental Study of a Stacked Lithium Niobate Transducer

Takeshi MORITA*, Toshiki NIINO[1], Hajime ASAMA and Hideo TASHIRO

Advanced Engineering Center, RIKEN (The Institute of Physical and Chemical Research), 2-1 Wako, Hirosawa, Saitama 351-0198, Japan
[1]*Institute of Industrial Science, The University of Tokyo, 7-22-1 Roppongi, Minato-ku, Tokyo 106-8558, Japan*

(Received November 23, 2000; accepted for publication January 17, 2001)

Generally, a lead zirconate titanate ceramic is utilized for a high-power transducer such as an ultrasonic motor drive. However, it is difficult to realize an ultrasonic motor that can withstand a high temperature, above 500°C. We focused on lithium niobate because it has a high Curie temperature (1210°C) and high quality factor. The electromechanical coupling factor of lithium niobate is large, although the permittivity is one hundred times smaller compared to that of hard-type lead zirconate titanate (PZT)-8. Hence a stacked structure is required to generate high output power. Dimensions of the fabricated actuator were 10 mm square and 18.5 mm long. The number of lithium niobate layers was 18. The calculated force factor of this transducer was 0.28 N/V, a value comparable to that of the bolted Langevin transducer using PZT, though the vibration velocity was saturated at 0.12 m/s. To realize improved transducer performance, we are attempting to fabricate a new transducer that can generate high vibration velocity.

KEYWORDS: extreme conditions lithium niobate, force factor, equivalent circuit, high-power transducer

Introduction

An ultrasonic motor has many advantages compared to conventional electromagnetic motors, for example, high-power density, brakeless construction and simple construction.[1)] However, few ultrasonic motors have been applied for practical use. The reason is that an electromagnetic motor displays similar advantages in small devices. For example, the advantage of low-speed high torque can be easily realized even in an electromagnetic-type motor by the use of a speed reducer.

Therefore, the research on ultrasonic motors should focus on specific applications that conventional electromagnetic motors cannot achieve. For example, if an ultrasonic motor can operate under extreme conditions such as ultrahigh vacuum,[2)] high temperature, low temperature and microfield,[3)] it could be practically applied. Withstanding such extreme conditions would render it indispensable for fundamental physical and chemical research studies. Actuators that can withstand extreme conditions will be useful in space or deep sea applications.

From these points of view, we investigated a driving source for an ultrasonic motor that can withstand high temperatures. The Curie temperature of a hard-type lead zirconate titanate (PZT) is about 300°C so that under the environment of 150°C or higher, the motor characteristic may deteriorate significantly. To realize a specific ultrasonic motor driven under a high temperature, over 500°C, we considered lithium niobate. The Curie temperature of lithium niobate is 1210°C, and the electromechanical coupling coefficient is relatively large, which is similar to that of PZT. Furthermore, vibration performance is superior because the quality factor is higher than 10^5. Lithium niobate should be focused on as a lead-free material from the viewpoint of environmental protection.[4)]

Previously, several researchers developed superior actuators using lithium niobate. Ishii *et al.* reported on a hybrid transducer ultrasonic motor using lithium niobate.[5)] They reported us that this motor was successfully driven but that precise characteristics under high temperature were not measured;[6)] the vibration measurements and driving results are not mentioned in ref. 5. A surface acoustic-wave motor, which is one type of ultrasonic motors, was investigated by Kurosawa.[7)] He utilized 128° Y-rotated lithium niobate for exciting a surface acoustic wave. His surface acoustic-wave motor would be useful if it could withstand high-temperature conditions. Nakamura *et al.* reported on a stacked actuator using the lithium niobate transverse effect for large displacement.[8)] The construction and cut angle are different from those of our transducer. They succeeded in demonstrating large and nonhysterisis displacement. Lithium niobate is a single crystal and thus no creep phenomenon was observed. Their actuator was very interesting, however, they did not research it as a high-power transducer.

In this paper, the fundamental analysis of the experimental and calculation results for stacked lithium niobate is discussed. The fabricated transducer will be utilized as a driving source for an ultrasonic motor that can withstand high temperatures. The target is a hard-type ultrasonic vibrator such as a bolted Langevin transducer using PZT.

2. Fabrication Process and Equivalent Circuits

As is well known, lithium niobate is an anisotropic single crystal and the cut angle strongly reflects the vibration performance. To generate high-power output, a stacked actuator was designed, namely, the thickness vibration of the thin plate is considered. The effective cut angle to generate the thickness vibration is 36° Y-cut X-propagation, as previously reported.[5)] The coupling factor, permittivity and piezoelectric coefficient of 36° Y-cut X-propagation lithium niobate are shown with a hard-type PZT-8 in Table I. Regarding the parameters for 36° Y-cut X-propagation lithium niobate, the thickness direction is expressed as 3.

The piezoelectric coefficient is about six times smaller than that of PZT-8. However, its suitability as a vibration source is not solely determined from the piezoelectric coefficient. For example, Hirose *et al.* researched the high-power characteristics of a PZT plate and reported that the mechanical loss became markedly larger for larger vibrational velocity, above

*Present address: Ceramics Laboratory, DMX-LC, Swiss Federal Institute of Technology-EPFL, CH-1015 Lausanne, Switzerland. E-mail address: takeshi.morita@epfl.ch

0.2 m/s.[9] It is also one of our goals to research the vibration velocity of stacked lithium niobate.

When a stacked transducer is fabricated, the impedance matching between lithium niobate and electrodes is very important because impedance missmatch results in a low quality factor. Fortunately, the acoustic impedance of lithium niobate is almost the same as that of brass. The acoustic impedance for 36° Y-cut X-propagation lithium niobate is 29.3×10^6 kg/ms and that of brass is 29.1×10^6 kg/ms. The two values have more than 99% correspondence.

The fabricated actuator is shown in Fig. 1. As discussed before, the driving vibration mode was the fundamental longitudinal mode. The dimensions of lithium niobate were 10 mm square and 0.5 mm thickness. The electrodes, which were made of brass, were similar in size to those of lithium niobate. To connect other electrodes, a small projection was fabricated on each electrode. Lithium niobate plates and brass electrodes were stacked with electroconductive adhesive (DOTITE FA705A) in order for the polarization directions to be mutually opposite. The projections of the electrodes were also alternatively aligned. The electroconductive adhesive was hardened at a high temperature (150°C) for 1 h. The thickness of the adhesive layers was about 10 μm.

As in the case of manufacturing stacked PZT, it is necessary to connect the electrodes at one-layer intervals. In this investigation, "Torr Seal" marketed by *Varian Co., Ltd.* was utilized as an insulator of the side surface. "Torr Seal" is an epoxy resin that is used as a vacuum seal and it resembles a ceramic after hardening. The guaranteed temperature range is up to 120°C. This paper deals with the fundamental vibration performance of the stacked lithium niobate transducer at room temperature. In the future, we will attempt to use sprayed alumina as an insulator that can withstand a much higher temperature.

After fabrication of the insulator, the insulator surface was ground with sandpaper until the electrode projection reached the surface. Each projection and electric wire was connected with electroconductive adhesive again.

Table I. Comparison between 36° Y-cut X-propagation $LiNbO_3$ and PZT-8. The thickness direction is expressed as 3 for lithium niobate.

	$LiNbO_3$	PZT-8
k_{33}	0.57	0.64
$\varepsilon_{33}/\varepsilon_0$	40	1000
e_{33} [C/m^2]	4.7	16.4
d_{33} [pC/N]	38.8	225
T_c [°C]	1210	300

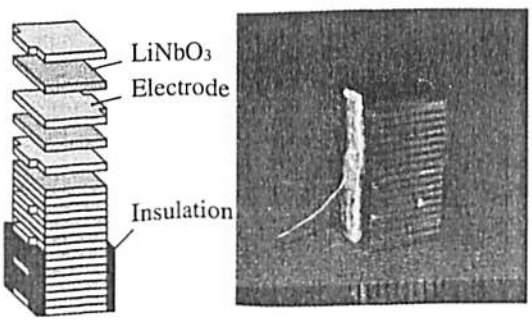

Fig. 1. Stacked actuator using lithium niobate.

To estimate the output force and vibration velocity, an equivalent circuit was effective. First, a modified Mason's equivalent circuit was considered for 0.5-mm-thick lithium niobate and a brass electrode. Regarding the modification of Mason's equivalent circuit, please refer to appendix A. The equivalent circuits were connected in series, as illustrated in Fig. 2(a). The boundary condition of both free ends is equal to that in the case of a one-free-end and a one-end-fixed half-length transducer. With this cascaded equivalent circuit, the force factor A was calculated to be 0.28 N/V.

In this equivalent circuit, however, the equivalent dumping coefficients are not included. The calculated vibration amplitude at the resonance frequency becomes infinity. Thus the cascade-connected equivalent circuit was used only for the force factor and resonance frequency calculations. The conventional equivalent circuit shown in Fig. 2(b), was constructed by using this force factor and resonance frequency.

Regarding the calculation method for equivalent mass L_m, please refer to appendix B. The equivalent compliance coefficient, C_m, could be obtained easily from the equation

$$C_m = \frac{1}{\omega_r^2 L_m}, \tag{1}$$

where ω_r is the angular velocity at the resonance frequency.

The equivalent damping coefficient R_m, is expressed as

$$R_m = \frac{\omega_r L_m}{Q}, \tag{2}$$

where Q is the quality factor. It is very difficult to estimate the quality factor without experimentation, thus the experimental results were utilized. Using the experimental quality factor, the vibration velocity v at the resonance frequency was estimated by the equation

$$v = \frac{AV}{R_m}, \tag{3}$$

where V is the input voltage.

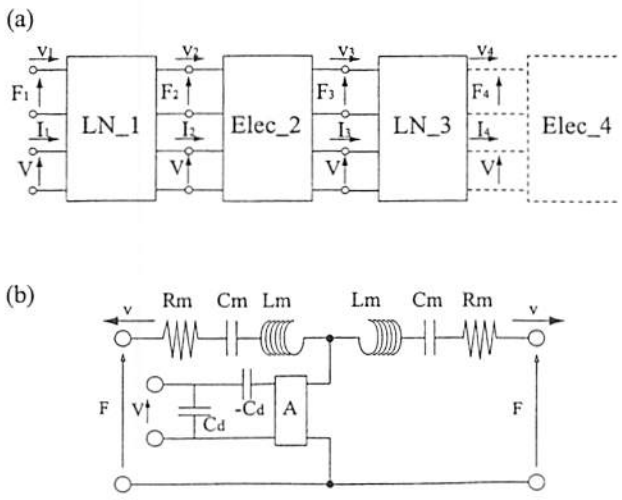

Fig. 2. Modified Mason's equivalent circuit in series (a) and a general equivalent circuit for piezoelectric transducer (b).

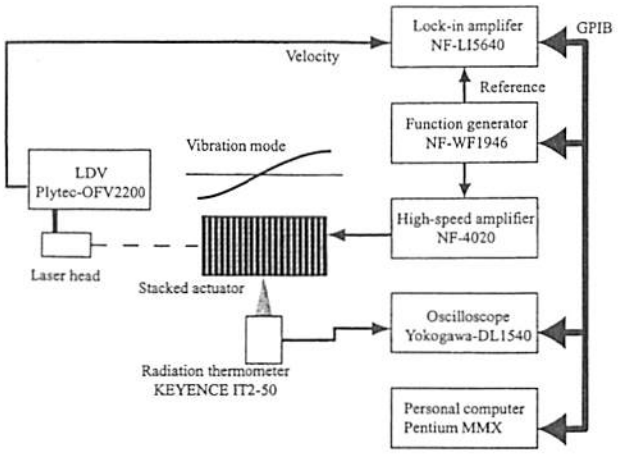

Fig. 3. Setup to measure the vibration velocity and temperature.

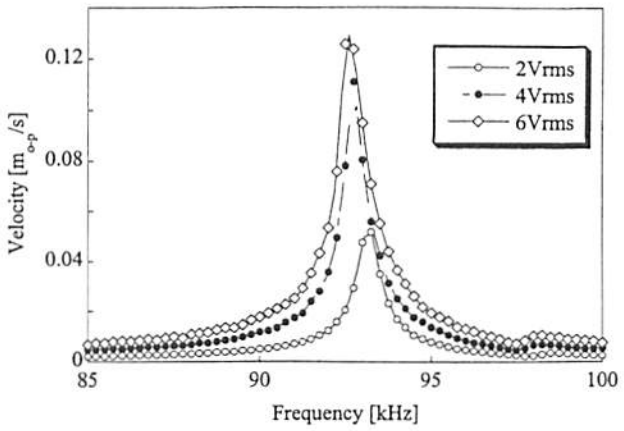

Fig. 4. Relationship between driving frequency and velocity for various input voltages.

3. Measurements

The vibration performance of the fabricated transducer was measured. The experimental setup is shown in Fig. 3. The driving source was generated with a function generator (NF WF1946) and applied to the transducer through a high-speed amplifier (NF 4020). The vibration velocity was measured with a laser Doppler velocimeter (PI-Polytec OFV2200). The excited vibration mode was in the longitudinal direction and the laser was irradiated at the top of the actuator. The transducer was placed on a soft material so as not to obstruct the vibration. The output signal was analyzed with a lock-in amplifier (NF-LI5640) using a reference signal from the function generator. During the measurement of the vibration velocity, the temperature at the center was also measured with a radiation thermometer (KEYENCE IT2-50). The output signal from the radiation thermometer was connected to an oscilloscope (Yokogawa DL1540) for analysis with a personal computer (Pentium MMX). The function generator, the lock-in amplifier and the oscilloscope were controlled by the personal computer with a general purpose interface bus (GPIB).

The result of the relationship between the driving frequency and the vibration velocity under various driving voltages is shown in Fig. 4. The resonance frequency was about 93 kHz. Under this velocity level, the resonance curve was symmetric. Usually, a jumping phenomenon is observed in the experiment of the high-power transducer using PZT,[9,10] although such a phenomenon was not observed experimentally here. Under the present condition, the vibration amplitude is not very large; hence it is unclear whether the lithium niobate could demonstrate linear performance under high-power output. In the next investigation using an improved transducer, we will attempt to research the nonlinearity of lithium niobate.

The relationship between the driving voltage and the vibration velocity or quality factor is shown in Figs. 5 and 6. The calculated velocity is also shown in this graph. The quality factor was calculated by fitting the measured data to the equivalent circuit.

These results show that the vibration velocity saturated at 0.12 m/s. This saturation comes from the decrease of the quality factor. The quality factor was 170 at the driving voltage of 1.0 V_{rms}. With the increase of the driving voltage, the vibration velocity decreased according to decrease of quality

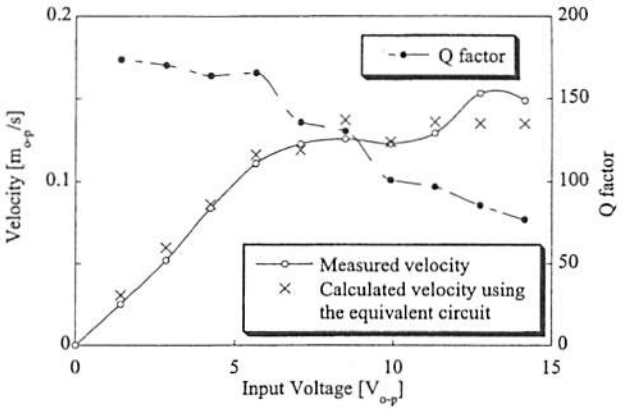

Fig. 5. Relationship between driving voltage, velocity and quality factor. Calculated data using an equivalent circuit is also given.

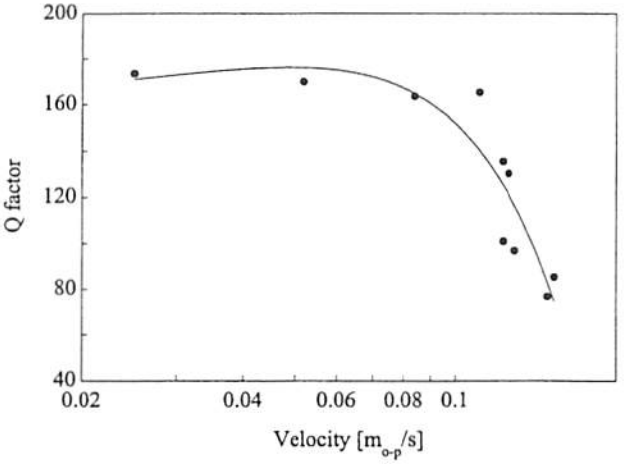

Fig. 6. Relationship between velocity and quality factor.

factor. The original quality factor of lithium niobate is more than 10^5; however, the measured quality factor is influenced by various factors, for example, the quality factor of the electrode, adhesive layer or insulator of the side surface.

The agreement between measured and calculated data indicated that the equivalent circuit is appropriate. Hence, the force factor of the fabricated transducer was 0.28 N/V. The force factor is proportional to the square of the output surface. The force factor per unit square, namely, 2.8 mN/V/m^2

matches that of the conventional bolted Langevin transducer using PZT.[11] From the viewpoint of electric field intensity, it is possible to increase the input voltage by more than one digit because the required electric field was only 10 V/mm to generate 0.12 m/s. Furthermore, the maximum temperature rise during all experiments was below 3°C.

The main problem with the fabricated transducer is the decrease in the quality factor. If the vibration velocity is not saturated and is increased to a larger value, this transducer could be utilized as a high-power transducer.

4. Conclusions

To realize an ultrasonic motor driven under high-temperature conditions, the high Curie temperature of lithium niobate was focused on. The 36° Y-cut X-propagation lithium niobate plates were stacked with the brass electrodes. The dimensions of each plate were $10 \times 10 \times 0.5\,\mathrm{mm}^3$. Brass was selected due to its suitable of acoustic impedance matching. The stacking number was 18 and the dimensions of the transducer were $10 \times 10 \times 18.5\,\mathrm{mm}^3$.

The vibration characteristics for this transducer were measured with a laser Doppler velocimeter. The quality factor was about 170 at a small input voltage. This value is very small compared to the original quality factor of lithium niobate. The reason for the small quality factor may be the adhesive layer. The vibration velocity increased with a larger input voltage, although it saturated at 0.12 m/s.

An equivalent circuit was constructed for this transducer. The force factor was 0.28 N/V, this value is appropriate because the experimental results and calculated ones demonstrated good agreement. The output force per unit voltage was comparable with that of the bolted Langevin transducer. Under the current conditions, the problem is that of vibration velocity saturation. The maximum velocity of the conventional bolted Langevin transducer was about 1 m/s in the catalog data.[11] To compete with such a high-power PZT transducer, the velocity saturation must be overcome. From the viewpoint of temperature rise and electric field intensity, it is possible. If this problem can be overcome, a high-power transducer may be realized.

We are currently attempting to improve the structure of the transducer for obtaining a higher quality factor. The main reason for the low quality factor and the decrease of the quality factor may be the adhesive layer, thus the improved transducer must be fabricated without adhesion. Utilizing the improved transducer, an ultrasonic motor can be fabricated and driven under high-temperature conditions.

Acknowledgements

The authors thank Dr. Ishii of the Tokyo Institute Technology and Professor Nakamura of Tohoku University for useful discussions.

1) S. Ueha and Y. Tomikawa: *Ultrasonic Motors Theory and Applications* (Oxford Science Publications, 1993) p. 4.
2) T. Morita, T. Niino and H. Aama: to be published in Proc. of IEEE Ultrason. Symp. 3B-4 (2000).
3) T. Morita, M. K. Kurosawa and T. Higuchi: Sens. & Actuators A83 (2000) 225.
4) Y. Jouno and Y. Tomikawa: Jpn. J. Appl. Phys. 39 (2000) 5619.
5) T. Ishii, K. Ohnishi and S. Ueha: Proc. of Acoustic Society of Japan Annu. Meet. (1-1-20) (1993) p. 921 [in Japanese].
6) Dr. Takaaki Ishii: private communication.
7) M. K. Kurosawa: Ultrasonics 38, Issues 1–8 (2000) 15.
8) K. Nakamura, Y. Adachi and T. Sakano: Proc. of Annu. IECIE Spring Meet. (1990) 1–353 [in Japanese].
9) S. Hirose, M. Aoyagi, Y. Tomikawa, S. Takahashi and K. Uchino: Ultrasonics 34 (1996) 213.
10) N. Aurelle, D. Guyamar, C. Richard, P. Gonnard and L. Eyaud: Ultrasonics 34 (1996) 187.
11) NGK-NTK (Nihon Tokushu Tougyou) catalogs for bolted Langevin transducer [in Japanese].
12) *Danseihasoshi-Handbook* (Ohm-sha, Tokyo, 1999) p. 103 [in Japanese].

Appendix A

Generally, Mason's equivalent circuit[12] is used to analyze piezoelectric excitation. The relationship between related parameters is expressed as

$$\begin{pmatrix} F_1 \\ F_2 \\ V \end{pmatrix} = \begin{pmatrix} \dfrac{\bar{Z}_0}{j\tan k_0 l} & \dfrac{\bar{Z}_0}{j\sin k_0 l} & \dfrac{e_{33}}{j\omega\varepsilon_{33}^S} \\ \dfrac{\bar{Z}_0}{j\sin k_0 l} & \dfrac{\bar{Z}_0}{j\tan k_0 l} & \dfrac{e_{33}}{j\omega\varepsilon_{33}^S} \\ \dfrac{e_{33}}{j\omega\varepsilon_{33}^S} & \dfrac{e_{33}}{j\omega\varepsilon_{33}^S} & \dfrac{1}{j\omega C_d} \end{pmatrix} \begin{pmatrix} v_1 \\ v_2 \\ I \end{pmatrix}, \tag{A·1}$$

where $\bar{Z}_0 = S\sqrt{\rho c^D}$, $k_0 = \frac{\omega}{c^D}$, $C_d = \frac{\varepsilon^S S}{l}$, S: section area, ρ: density, c^D: stiffness, ω: angular velocity, ε: permittivity and l: thickness; The left-hand side of this matrix expresses force and voltage for ports 1 and 2 and the right-hand side expresses velocity and current. In this expression, it is difficult to connect it in series. Hence we modified Mason's equivalent circuit as shown in Fig. A·1(a). The matrix expression is transformed to

$$\begin{pmatrix} F_{i+1} \\ v_{i+1} \\ V \\ I_{i+1} \end{pmatrix} = \begin{pmatrix} \frac{c^2-ad}{c^2-bd} & \frac{(a-b)((a+b)d-2c^2)}{c^2-bd} & \frac{c(a-b)}{c^2-bd} & 0 \\ \frac{d}{c^2-bd} & \frac{c^2-ad}{c^2-bd} & -\frac{c}{c^2-bd} & 0 \\ 0 & 0 & 1 & 0 \\ \frac{c}{c^2-bd} & -\frac{ac-bc}{c^2-bd} & -\frac{b}{c^2-bd} & 1 \end{pmatrix} \begin{pmatrix} F_i \\ v_i \\ V \\ I_i \end{pmatrix}, \quad \text{(A·2)}$$

where

$$a = \frac{\tilde{Z}_0}{j \tan k_0 l}, \quad b = \frac{\tilde{Z}_0}{j \sin k_0 l}, \quad c = \frac{e_{33}}{j\omega\varepsilon_{33}^S}, \quad d = \frac{1}{j\omega C_d}.$$

If the considered material has no piezoelectric effect, such as an electrode, the eq. (A·2) is transformed as

$$\begin{pmatrix} F_{i+1} \\ v_{i+1} \\ V \\ I_{i+1} \end{pmatrix} = \begin{pmatrix} \frac{a}{b} & -\frac{a^2-b^2}{b} & 0 & 0 \\ -\frac{1}{b} & \frac{a}{b} & 0 & 0 \\ 0 & 0 & 1 & 0 \\ 0 & 0 & 0 & 1 \end{pmatrix} \begin{pmatrix} F_i \\ v_i \\ V \\ I_i \end{pmatrix}. \quad \text{(A·3)}$$

The equivalent circuit is shown in Fig. A·1(b). Of course, the parameters, for example a and b involved in eq. (A·3) should be changed to those for the electrode. The stacked transducer is expressed with the connected equivalent circuits as shown in Fig. 2(a). Regarding the matrix expression, it is sufficient to multiply eqs. (A·2) and (A·3) by the layer number. Using the boundary conditions, the relationship between the output velocities, output forces, input voltage and input currents is clarified. Consequently, from the proportional coefficient between input voltage and output force, the force factor can be obtained.

Appendix B

To calculate equivalent mass for a conventional equivalent circuit as shown in Fig. 2(b), the vibration distribution should be considered. If the transducer is composed of the same material and the longitudinal vibration mode was excited, the equivalent mass (L_m) can be easily obtained by

$$M(= L_m) = \int_0^{L/2} S\rho \sin^2\left(2\pi \frac{x}{\lambda}\right) dx, \quad \text{(B·1)}$$

where S: sectional area, ρ: density and λ: wavelength. In the equivalent circuit, the mechanical part is divided into two parts thus the integration range starts from 0.

When different materials were stacked together and their acoustic impedance was equal, the vibration phase (x/λ) is kept on continuously in the verge of two materials. In this appendix, the different materials are referred to as material A and material B. The excited vibration mode is the symmetric longitudinal mode, thus it is sufficient to discuss the half-length of the transducer. In this situation, the boundary condition becomes a free end and a fix condition.

The fixed material is assumed to be material A. One surface is fixed and the other face is connected to material B. Thus the equivalent mass for the first layer M_1 is calculated as

$$M_1 = \int_0^{L_A} S\rho_A \sin^2\left(2\pi \frac{x}{\lambda_A}\right) dx, \quad \text{(B·2)}$$

where $\lambda_A = \frac{v_A}{f_r}$, f_r: resonance frequency and v_A: peculiar longitudinal velocity. Subscript A means that the parameter is for material A. The next layer is of material B. We should consider the range of integration. In eq. (B·2), the last point of the integration is L_A, which means that the vibration phase corresponds to $2\pi \frac{L_A}{\lambda_A}$. Hence, the next starting point x_{start}

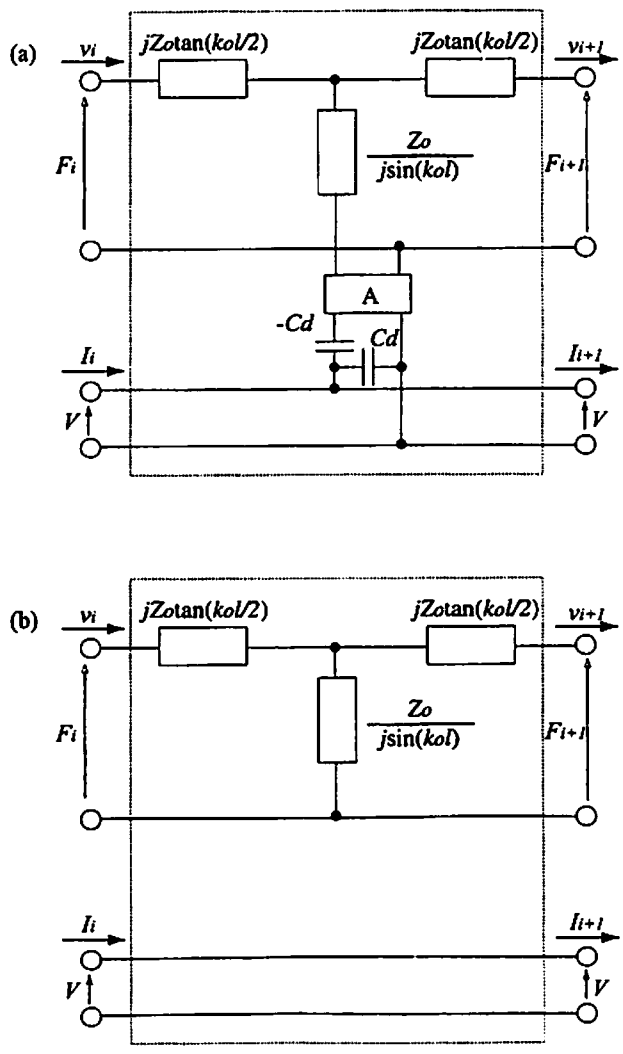

Fig. A·1. Modified Mason's equivalent circuits for piezoelectric layer (a) and no piezoelectric layer (b).

could be obtained with

$$\frac{2\pi}{\lambda_A}L_A = \frac{2\pi}{\lambda_B}x_{start}$$

$$x_{start} = \frac{\lambda_B}{\lambda_A}L_A. \tag{B·3}$$

This calculation is performed under the condition of equal acoustic impedance between two materials. When the acoustic impedance is different, the starting point of integration is expressed as

$$x_{start} = \frac{\lambda_B}{2\pi}\tan^{-1}\left[\frac{Y_B\lambda_A}{Y_A\lambda_B}\tan\left(\frac{2\pi}{\lambda_A}L_A\right)\right], \tag{B·4}$$

where Y_A and Y_A are the Young's moduli for each material. This expression is obtained by considering the continuousness of the vibration velocity and the stress. The equivalent mass of second layer M_2 is integrated over the range of

$$\frac{\lambda_B}{\lambda_A}L_A \le x \le \frac{\lambda_B}{\lambda_A}L_A + L_B \tag{B·5}$$

.nd

$$M_2 = \int_{\frac{\lambda_B}{\lambda_A}L_A}^{\frac{\lambda_B}{\lambda_A}L_A+L_B} S\rho_B \sin^2\left(2\pi\frac{x}{\lambda_B}\right)dx. \tag{B·6}$$

is obtained.

Regarding the next equivalent mass M_3, the range of integration is

$$L_A + \frac{\lambda_A}{\lambda_B}L_B \le x \le 2L_A + \frac{\lambda_A}{\lambda_B}L_B \tag{B·7}$$

With the same consideration, the relationship regarding integration range is gained inductively as follows

$$\left(\frac{i-1}{2}\right)\left(L_A + \frac{\lambda_A}{\lambda_B}L_B\right) \le x \le \left(\frac{i-1}{2}\right) \times \left(L_A + \frac{\lambda_A}{\lambda_B}L_B\right) + L_A \quad (\textit{for } i \in \textit{odd, material } A)$$

$$\frac{i}{2}\frac{\lambda_B}{\lambda_A}L_A + \left(\frac{i}{2} - 1\right)L_B \le x \le \frac{i}{2}\left(\frac{\lambda_B}{\lambda_A}L_A + L_B\right)$$

$$(\textit{for } i \in \textit{even, material } B). \tag{B·8}$$

By repeating the integration calculation as in eqs. (B·3) or (B·6), each equivalent mass can be obtained. Then, the total equivalent mass can be obtained by

$$L_m = \sum_{i=1}^{N/2} M_i, \tag{B·9}$$

where N is the stacking number.